

A REDUCED ORDER MODEL OF TAUT CABLE DYNAMICS USING KARHUNEN-LOEVE DECOMPOSITION

**Mario R. Escalante^{a,b}, Omar R. Faure^{a,b}, Viviana C. Rougier^{a,b},
Marta B. Rosales^{c,d} and Carlos P. Filipich^{c,e}**

^aGMN, F. R. C. del Uruguay, Universidad Tecnológica Nacional,
Ing Pereyra 676, 3260 Concepción del Uruguay, Argentina
mescalante@frcu.utn.edu.ar, ofaure@frcu.utn.edu.ar, rougierv@frcu.utn.edu.ar

^bF. R. Concordia, Universidad Tecnológica Nacional, Salta 277, 3200 Concordia, Argentina

^cDepartamento de Ingeniería, Universidad Nacional del Sur, Alem 1253, 8000 Bahía Blanca,
Argentina, *mrosales@criba.edu.ar*

^dCONICET, Argentina

^eCIMTA. Fac. Reg. Bahía Blanca, Universidad Tecnológica Nacional, 8000 Bahía Blanca, Argentina, *cfilipich@gmail.com*.

Keywords: taut cables, reduced order model, proper orthogonal decomposition, Karhunen-Loeve decomposition.

Abstract. In a previous work carried out by the research group, the dynamics of slack extensible cables subjected to end prescribed motion was tackled through a reduced order model with a Karhunen-Loeve (KL) basis (also known as POMs, Proper Orthogonal modes). The latter was found from data of the dynamic response of an inextensible chain under similar conditions. The use of the chain problem was a natural selection due to the similarity between the slack cable and the chain. Now, the same approach is applied to a taut cable which exhibits small sag. Here, the pretension level is higher, the extensibility is more noticeable and the range of validity of the chain basis should be verified. In the present work, both the chain and the cable will be exposed to horizontal forces and prescribed dynamic motion at the ends. This situation resembles the case of the guys in a guyed structure as in the case of communications towers. The chain dynamics are solved with two DAE approaches and then, the KL basis extracted from the obtained data. It should be mentioned that this basis is optimal for the problem under study, in the sense of the least squares criterion. Once the basis is found along with the eigenvalues (POVs, Proper Orthogonal values, sometimes named "energy"), the POMs are introduced in a Galerkin approach to represent the dynamics of the extensible cables. Given its hierarchical grouping, the KL decomposition allows to choose only a few modes to be used in a Galerkin approximation, keeping the most important component of the dynamic response information. An illustrative example is worked out using the data from a real communication tower guy. The availability of a reduced dimensional model is very useful for structures that have large or infinite degrees of freedom. The advantages are apparent: considerable saving of computing times makes simulations more economical and parametric and bifurcation studies feasible.

1 INTRODUCTION

Structural cables constitute an important part of modern structural engineering applications involving large spans. Pretensioned guy cables are implemented in radio and communication guyed towers to provide stability and support to flexible masts reaching high elevations as they are subjected to the effect of wind-induced forces.

Centuries ago, researchers studied the subject of a vibrating taut string and used experimental techniques to find the laws describing its behavior. Over the years, mathematical models describing string vibrations were established. Cable dynamics include free vibration, response to forcing excitation and experimental measurements of cable vibrations. In recent years, attention has been focused the methods of analyzing guyed towers. Ordinary structural analysis does not yield reasonable solutions. The highly nonlinear tension-chord elongation relationship of guy cable introduces geometrical nonlinearities when the mast experiences lateral displacements.

In the dynamic analysis of cable systems, superposition of loads and displacements is not strictly valid due to the effects of loading nonlinearities and large amplitude vibrations. In general, the governing equations for pre-tensioned cable dynamics are coupled and highly nonlinear. General analytical solutions for these systems are not available, and therefore, numerical techniques have to be used, e.g., the finite element method (FEM), and the finite difference method (FDM).

A historical review of cable dynamics, along with a summary of recent contributions specific to suspended cables can be found in Irvine (1981) and Triantafyllou, (1984, 1987). The prominent linear theory developed by Irvine and Caughey (1974) describes the free vibration of a suspended cable about a planar equilibrium with small sag and horizontal supports. Hagedorn and Shafer (1980) were the first to extend the (in-plane) linear theory to account for geometric nonlinearities. Free planar, nonlinear cable oscillations were further studied in by Rega and Luongo (1980), Rega *et al.* (1980), Luongo *et al.* (1984) and Takahashi and Konishi (1987). Recently nonlinear modelling, analysis and phenomena are comprehensively addressed in the review papers by Rega (2004) and Ibrahim (2004) concerned with deterministic and stochastic dynamics, respectively.

The authors have been working in dynamics of cables using a quasi-static model for the cables with different complexities (Rosales *et al.*, 2003; Escalante *et al.*, 2005). In a previous work of the research group, the dynamics of slack extensible cables subjected to end prescribed motion (Escalante *et al.*, ENIEF 2008) was approached through a reduced order model with a Karhunen-Loeve (KL) basis by means of the proper orthogonal decomposition (POD). The latter was found from the data of the dynamic response of an inextensible chain under similar conditions. The use of the chain problem was a natural selection due to the similarity between the slack cable and the chain.

In the present work, the same approach is applied to a taut cable which exhibits small sag, where both the chain and the cable are now assumed to be elastic and will be exposed to arbitrary loads that may arise from several sources, including self-

weight and wind pressures.

The proper orthogonal decomposition (POD) is a powerful and elegant method for data analysis aimed at obtaining low-dimensional approximate descriptions of a high-dimensional process. The POD provides a basis for the modal decomposition of an ensemble functions, such as data obtained in the course of experiments or numerical simulations. Its properties suggest that it is the preferred basis to use in various applications. The basis functions are commonly called empirical eigenfunctions, empirical basis functions, empirical orthogonal functions, proper orthogonal modes (POMs), or basis vectors. The most striking feature of the POD is its optimality: it provides the most efficient way of capturing the dominant components of an infinite-dimensional process with only a finite number of "modes", and often surprisingly few "modes" (Chatterjee, 2000; Holmes *et al.*, 1996).

In general there are two interpretations for the POD. The first interpretation regards the POD as the Karhunen-Loève decomposition (KLD) and the second one considers that the POD consists of three methods: the KLD, the principal component analysis (PCA), and the singular value decomposition (SVD). The first interpretation appears in many engineering literatures related to the POD. An interesting analysis about the equivalence among the three methods can be found in Liang *et al.* (2002).

The POD was independently developed by several researchers including Karhunen (1946), Kosambi (1943), Loève (1948), Obukhov (1954) and Pougachev (1953), and was originally conceived in the framework of continuous second-order processes. When restricted to a finite dimensional case and truncated after a few terms, the POD is equivalent to principal component analysis (PCA). This latter methodology originated with the work of Pearson (1901), as a means of fitting planes by orthogonal least squares but was also proposed by Hotelling (1933)

It is emphasized that the KLD has become a well-established method in various fields of scientific research ranging from biological, meteorological and seismological to engineering applications (Kerschen *et al.*, 2005; Glösmann and Kreuzer, 2005). The method appears in various fields in the literature and is known by other names depending on the area of application, namely PCA in the statistical literature, empirical orthogonal function in oceanography and meteorology, and factor analysis in psychology and economics.

In the present work, both the chain and the cable are assumed to be elastic and will be exposed to horizontal forces and prescribed dynamic motion at the ends. This situation resembles the case of the guys in a guyed structure as in the case of communications towers.

The nonlinear static analysis of the cable subjected to static loading is performed by solving the classical catenary equation (Leonard, 1988) and also for comparison, like an elastic chain involving several point masses connected by elastic springs which can only support tension (Wilson *et al.*, 2003).

The chain dynamics are solved by modeling an elastic chain involving several point masses connected by elastic springs which can only support tension, then the KL ba-

sis are extracted from the obtained data. Once the basis is found along with the eigenvalues (POVs, Proper Orthogonal values, sometimes named "energy"), the POMs are introduced in a Galerkin approach to represent the dynamics of the extensible cables. Given its hierarchical grouping, the KL decomposition allows to select only a few modes to be used in a Galerkin approximation, keeping the most of the dynamic response information. An illustrative example is worked out using the data of a real communication tower guy. The availability of a reduced dimensional model is very useful for structures that have large or infinite degrees of freedom. The advantages are apparent: considerable saving of computing times makes on one hand, simulations more economical and on the other hand parametric and bifurcation studies feasible.

2 DYNAMICS OF ELASTIC CHAINS

In order to construct a low-order dynamical model to simulate the dynamical behavior of taut cables we analyze a simpler problem with similar characteristics, like an elastic chain. A Karhunen-Loève decomposition (KLD) is performed to obtain a basis which, is later introduced in a Galerkin approximation to solve the cable dynamics problem. This approach has advantages and limitations. As for the former, we could mention the simplicity of the reference problem and with respect to the latter, the dynamics of the cables should resemble that of the chain.

The mathematical model of interest is a two dimensional motion of a cable (or chain) having mass particles connected by springs. A chain having specified end motions illustrates the behavior of a system governed by nonlinear equations of motion.

The equations of motion are easy to formulate in terms of the horizontal and vertical coordinates of each mass. The dimensionality needed to handle the elastic chain is twice as much that needed for a similar rigid link model. Even if it is natural to utilize a three dimensional model, it is easy to simplify it for two dimensional motions.

Consider a chain having n mass particles $m_j, 1 \leq j \leq n$, connected by n springs having unstretched lengths $l_j, 1 \leq j \leq n$. The geometry is depicted in Figure 1

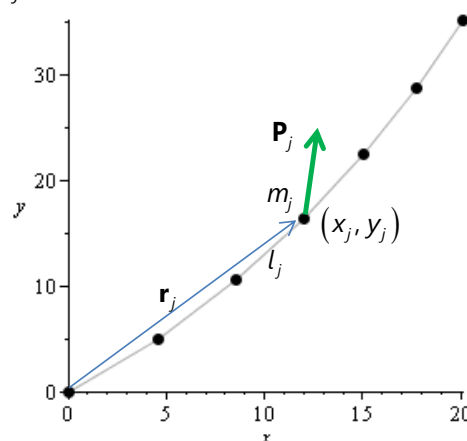


Figure 1: Chain geometry

The position of particle m_j is denoted by vector $\mathbf{r}_j(t) = [x_j(t), y_j(t)]$ with $\mathbf{r}_0(t)$ and $\mathbf{r}_{n+1}(t)$ denoting the outer end positions of the first and last mass particles, which are assumed to be known time functions. We assume that concentrated forces $\mathbf{P}_j(t)$ are applied to the particles. The tensile force in spring number j at the time t is given by

$$\mathbf{T}_j(t) = k_j(1 - l_j/L_j(t))\zeta_j(t)\mathbf{R}_j(t) \tag{1}$$

where $\zeta_j(t)$ is equal to 1 if $L_j(t) - l_j > 0$, else is 0,

$$\mathbf{R}_j(t) = \mathbf{r}_{j+1}(t) - \mathbf{r}_j(t), L_j(t) = \|\mathbf{R}_j(t)\| \tag{2}$$

and k_j denotes a spring constant. Then, the equations of motion are given by

$$\ddot{\mathbf{r}}_j = \mathbf{P}_j - \mathbf{T}_j + \mathbf{T}_{j-1} / m_j, \quad 1 \leq j \leq n \tag{3}$$

where dots denote differentiation with respect to t .

The equations are easy to state form using array operations. Furthermore, the two dimensional case can be simplified further by using complex numbers to represent the particle positions.

An algorithm to compute the response of a chain released from rest is reported in (Wilson *et al.*, 2003).

Initial conditions (IC) must be imposed to the coordinates involved in the governing equation (3), in our case $\mathbf{r}_j(0), \dot{\mathbf{r}}_j(0), j = 0, \dots, n$. These conditions are obtained from the geometry of the static solution of a catenary cable under self-weight.

3 STATIC ANALYSIS OF AN ELASTIC CABLE (CATENARY EQUATION)

The solution for the displacement of a nonsymmetrical sagged elastic cable has been known since at least the 1930s (Irvine,1981), it is not much necessary to derive it again from scratching here. However, as several components of the cable profile derivation are relevant to the work presented in this paper, we will briefly do it using our coordinate system and variables.

Nonlinear static model for cables can be developed by solving the classical catenary equation (Leonard, 1988). The profile of an inclined cable suspended under the influence of a uniform self-weight q is illustrated in Figure 2, where ρ_0 is the cable density material, L_0 is the unstrained length of the cable, E, Ω and ΔL represent the elastic modulus, the unstrained cross-sectional area, and the strain of the cable, respectively.

As shown in Figure 2, a point along the length of the strained cable can be denoted by the Cartesian coordinates x and y , and the path variables s . The variable s represents the strained length of the cable segment as measured from the attachment point of the cable to the point (x, y) . The variable S will be used to denote the unstrained length of that cable segment.

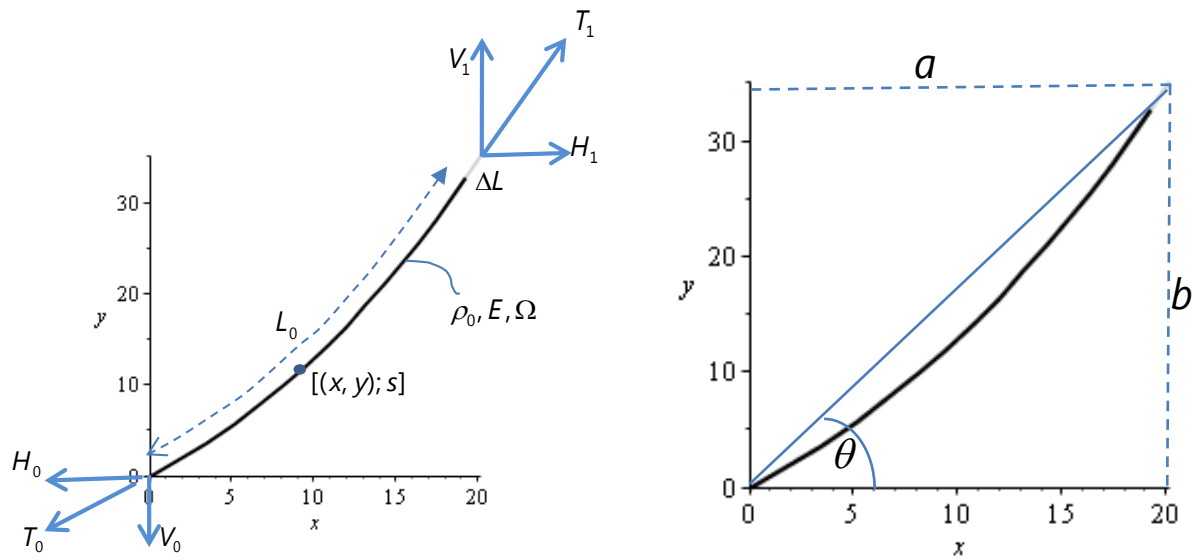


Figure 2: Diagram of sagged cable

From this starting point, the equations for the shape of the cable can be derived. The equilibrium of forces on a differential length, gives,

$$\frac{dH}{dx} = 0, \quad H = H_0, \quad (4)$$

$$\frac{dV}{dx} = -q \frac{ds}{dx}. \quad (5)$$

Also, since the tension direction is along the tangent to the arc,

$$V = H_0 \frac{dy}{dx}. \quad (6)$$

Using the derivatives of equations (5) y (6) and the fact that $ds^2 = dx^2 + dy^2$,

$$\frac{d^2y}{dx^2} + \frac{q}{H_0} \sqrt{1 + \left(\frac{dy}{dx}\right)^2} = 0. \quad (7)$$

The tension at any point (x, y) is given by,

$$T = H_0 \sqrt{1 + \left(\frac{dy}{dx}\right)^2}. \quad (8)$$

Integrating equation (7) twice and applying the boundary conditions, $y=0$ at $x=0$ and $y=a \tan \theta$ at $x=a$, leads to

$$y = \frac{H_0}{q} \left\{ \cosh(\zeta + \beta) - \cosh \left[\zeta + \beta \left(1 - 2 \frac{x}{a} \right) \right] \right\}. \quad (9)$$

The above equation is the classic catenary equation for the deflected profile y of the arc, where

$$\beta = \frac{qa}{2H_0}, \quad (10)$$

$$\zeta = \sinh^{-1} \left(\tan \theta \frac{\beta}{\sinh \beta} \right). \quad (11)$$

Substituting equation (9) into equations (6) and (8), vertical force and tension can be obtained as,

$$V = H_0 \sinh \left[\zeta + \beta \left(1 - 2 \frac{x}{a} \right) \right], \quad (12)$$

$$T = H_0 \cosh \left[\zeta + \beta \left(1 - 2 \frac{x}{a} \right) \right]. \quad (13)$$

The stretched length to a point x on the horizontal span is obtained from $ds = [1 + (dy/dx)^2]^{1/2} dx$ ($s = 0$ at $x = 0$) as,

$$\frac{s}{L} = \frac{V - V_0}{qa}, \quad (14)$$

where, V_0 is the vertical force at $x = 0$, and V is the vertical force at x .

The total unstretched length is determined from the differential equation

$$\frac{dS}{dx} = \frac{T/H_0}{1 + T/\Omega E} \approx \left(\frac{T}{H_0} \right) \left[1 - \frac{H_0 T}{E \Omega H_0} \right]. \quad (15)$$

Applying the boundary conditions $S = 0$ at $x = 0$ and $S = L_0$ at $x = a$ and integrating equation (15), the equation obtained is,

$$\frac{L_0}{L} = \frac{V_0 - V_1}{qa} - \frac{qa}{2E\Omega} \left[\frac{H_0}{qa} + \frac{V_0 T_0 - V_1 T_1}{(qa)^2} \right]. \quad (16)$$

Equations (9) to (16) describe the behavior of a catenary segment in terms of unknown horizontal force H_0 and self-weight q .

If the horizontal component of the force is calculated, the unstretched length of the cable can be calculated using equation (16). This is important because the only reference parameter that remains constant as the cable deforms is its unstretched length L_0 . Cable position is based on initial tension at the right end T , which is a specified input value. First an approximate value $H_0 \approx T_1 \cos \theta$ is calculated. From equation (13) at $x = a$, we obtain $T_1 = H_0 \cos(\zeta - \beta)$. This equation, used iteratively with equations (10) and (11), can be used to determine the initial value of horizontal force. L_0 can then be calculated from equation (16).

4 DYNAMICS OF EXTENSIBLE CABLES

Now, the dynamics of an extensible cable will be stated. Recall that the KLD will be performed by using the chain dynamics and after that, the KL basis will be introduced in a Galerkin approximation to find the cable response.

Figure 3 shows a free body diagram of a portion of a cable, in which the acting forces are the self weight and constant uniform forces q_h (horizontal) and q_v (vertical). Assuming that the cable is extensible, the equilibrium equations of a discrete portion

are:

$$\Delta H - \Delta r'' \dots X = 0, \tag{a}$$

$$\Delta V - \Delta r'' \dots g + q_v \Delta X = 0, \tag{b}$$

where dots indicate derivative with respect to the time variable, $\Delta mg = \rho_0 \Omega \Delta X = \rho \Omega \Delta s$, x^* and y^* are intermediate points, and if $\bar{\xi} = \Delta s / \Delta X$ (stretching) then $\rho_0 = \rho \bar{\xi}$. ρ is the cable density material, Ω is the cross section and g is the gravity acceleration.

Dividing each member by ΔX

$$\frac{\Delta H}{\Delta X} - \dots - q_h = 0, \tag{a}$$

$$\frac{\Delta V}{\Delta X} - \dots - \rho \Omega g + q_v = 0, \tag{b}$$

and assuming $\Delta X \rightarrow 0$, the local equations for the motion of the extensible cable under self-weight, are obtained :

$$H' = \rho \Omega \xi'' \dots \tag{a}$$

$$V' = \rho \Omega \xi (\dots - q_v), \tag{b}$$

primes indicate derivative with respect to X , $\xi = ds / dX$ and H and V are the horizontal and vertical components of the static cable tension T , respectively:

$$H = T \cos \theta = T \frac{dx}{ds} = \frac{T}{\xi} \frac{dx}{dX}, \tag{20}$$

$$V = T \sin \theta = T \frac{dy}{ds} = \frac{T}{\xi} \frac{dy}{dX}.$$

Let us now propose the following constitutive law for the cable material

$$\frac{T}{\xi} = K \frac{(\xi^2 - 1)}{2}, \tag{21}$$

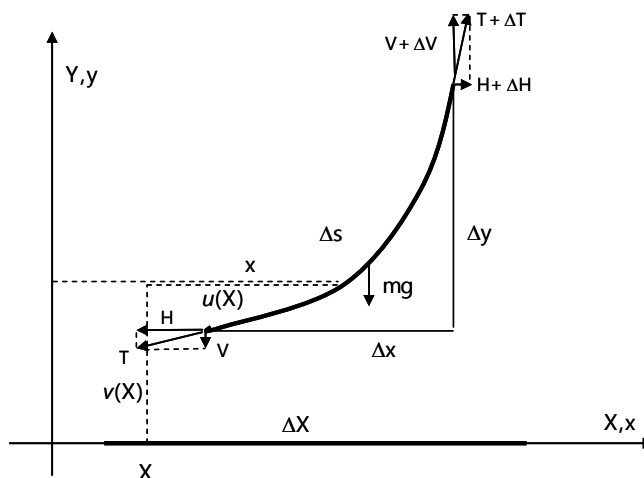


Figure 3: Free body diagram of a portion of cable

which was discussed in Filipich and Rosales (2000). Then Eqs. (19) can be written as follows:

$$\begin{aligned} \left(\frac{Tx'}{\xi} \right)' &= \rho_0 \Omega \ddot{\cdot} \dots \\ \left(\frac{Ty'}{\xi} \right)' &= \rho_0 \Omega (\ddot{\cdot} \dots, q_v) \end{aligned} \tag{22}$$

If K is a constant with axial stiffness unit, after rearranging, we obtain

$$\begin{aligned} [x'(\xi^2 - 1)]' &= \frac{2}{K} (\rho_0 \Omega \ddot{\cdot} \dots) \\ [y'(\xi^2 - 1)]' &= \frac{2}{K} (\rho_0 \Omega \ddot{\cdot} \dots, J - q_v) \end{aligned} \tag{23}$$

Equations (23) represent a nonlinear system of partial differential equations and its solution is tackled by means of the Galerkin Method using KL basis of the chain problem.

5 PROPER ORTHOGONAL DECOMPOSITION

Let $\theta(x, t)$ be a random field on a domain Ω . This field is first decomposed into mean $\mu(x)$ and time varying parts $\mathcal{G}(x, t)$:

$$\theta(x, t) = \mu(x) + \mathcal{G}(x, t) \tag{24}$$

At time t_k , the system displays a snapshot $\mathcal{G}^k(x) = \mathcal{G}(x, t_k)$. The POD aims at obtaining the most characteristic structure $\varphi(x)$ of an ensemble of snapshots of the field $\mathcal{G}(x, t)$ that maximizes the ensemble average of the inner products between $\mathcal{G}^k(x)$ and $\varphi(x)$:

$$\text{Maximize } \langle |\mathcal{G}^k, \varphi|^2 \rangle \text{ with } \|\varphi\|^2 = 1 \tag{25}$$

where $(f, g) = \int_{\Omega} f(x)g(x)d\Omega$ is the inner product in Ω ; $\langle \cdot \rangle$ denotes averaging;

$\|\cdot\| = (\cdot, \cdot)^{1/2}$ is the norm; $|\cdot|$ is the modulus. Holmes *et al.* (1996) show that the maximization reduces to the following integral eigenvalue problem

$$\int_{\Omega} \langle \mathcal{G}^k(x)\mathcal{G}^k(x') \rangle \varphi(x') dx' = \lambda \varphi(x) \tag{26}$$

Where $\langle \mathcal{G}^k(x)\mathcal{G}^k(x') \rangle$ is the averaged auto-correlation function. The solution of the optimization problem (25) is thus given by the orthogonal functions $\varphi_i(x)$ of the integral equation (26), called the proper orthogonal modes (POMs). The corresponding eigenvalues λ_i ($\lambda_i \geq 0$) are the proper orthogonal values (POVs). The POM associated with the greatest POV is the optimal vector to characterize the ensemble of

snapshots. The POM associated with the second greatest POV is the optimal vector to characterize the ensemble of snapshots but restricted to the space orthogonal to the first POM, and so forth. The energy \mathcal{E} contained in the data is defined as the sum of the POVs, i.e. $\mathcal{E} = \sum_j \lambda_j$, and the energy percentage captured by the i th POM is given by $\lambda_i / \sum_j \lambda_j$.

The POMs may thus be used as a basis for the decomposition of the field $\mathcal{G}(x, t)$:

$$\mathcal{G}(x, t) = \sum_{i=1}^{\infty} a_i(t) \varphi_i(x) \quad (27)$$

where the coefficients $a_i(t)$ are uncorrelated, i.e., $\langle a_{i(t)} a_{j(t)} \rangle = \delta_{ij} \lambda_i$, and are determined by $a_i(t) = (\mathcal{G}(x, t), \varphi_i(x))$.

5.1 Practical computation of the POD

In practice, the data are discretized in space and time. Accordingly, m observations of an n -dimensional vector \mathbf{x} are collected, and an $(n \times m)$ response matrix is formed:

$$\mathbf{X} = [\mathbf{x}_1, \dots, \dots] \begin{bmatrix} x_{11} & \dots & \dots \\ \vdots & \ddots & \vdots \\ x_{n1} & \dots & \dots \end{bmatrix} \quad (28)$$

Since the data are now discretized and do not necessarily have a zero mean, the averaged auto-correlation function is replaced by the covariance matrix $\mathbf{C}_v = E[(\mathbf{x} - \boldsymbol{\mu})(\mathbf{x} - \boldsymbol{\mu})^T]$, where $E[\cdot]$ is the expectation and $\boldsymbol{\mu} = E[\mathbf{x}]$ is the mean of the vector \mathbf{x} . The POMs and POVs are thus characterized by the eigensolutions of matrix \mathbf{S} . If data have a zero mean, an estimate of the covariance matrix is merely given by the following expression:

$$\mathbf{C}_v = \frac{1}{m} \mathbf{X} \mathbf{X}^T \quad (29)$$

It is emphasized that the POD can also be computed through the singular value decomposition of matrix \mathbf{X} :

$$\mathbf{X} = \mathbf{U} \boldsymbol{\Sigma} \mathbf{V}^T \quad (30)$$

where \mathbf{U} is an $(m \times m)$ orthonormal matrix containing the left singular vectors; $\boldsymbol{\Sigma}$ is an $(m \times n)$ pseudo-diagonal and semi-positive definite matrix with diagonal entries containing the singular values σ_i and \mathbf{V} is an $(n \times n)$ orthonormal matrix containing the right singular vectors.

The POMs, defined as the eigenvectors of the covariance matrix \mathbf{C}_v , are thus equal to the left singular vectors of \mathbf{X} . The POVs are the square of the singular values divided by the number of samples m . The main advantage in considering the SDV to compute the POD is that additional information is obtained through the matrix \mathbf{V} . The column \mathbf{v}_i of matrix \mathbf{V} contains the amplitude modulation of the corresponding

POM, normalized by the singular value σ_i . This information may also provide important insight into the system dynamics.

6 NUMERICAL EXAMPLES

6.1 Example 1

A cable of length L_0 with both ends fixed at $(0,0)$ and (a,b) respectively, is considered. The following data are adopted: $a=20.40\text{m}$, $b=57.70\text{m}$, $\Omega=1.25\times 10^{-4}\text{m}^2$, $\omega_x=0.1\text{rad/s}$, $\gamma_0=\rho_0g=78500\text{N/m}^3$, $f_1(t)=20.40+0.07(1-\cos(\omega_x t))$, $f_2(t)=0$, $E=1.6\times 10^{11}\text{N/m}^2$. The algorithm derived in Section 3 was implemented to obtain the geometric configuration of the static solution of a cable under self-weight and a pretension T_1 . Results can be seen in Table 1, where the unstretched and stretched length, and strain are shown.

Tensión [$\overline{\text{kg/cm}^2}$]	T_1 [N]	L_0 [m]	L [m]	ΔL [m]	T_0 [N]
150	1875	61.2367	61.2416	0.005	1308
300	3750	60.1479	61.2086	1.061	3183
600	7500	58.9937	61.2020	2.208	6933
1200	15000	56.6972	61.2005	4.503	14433

Table 1: Stretched and unstretched length, and strain of a suspended cable supported at the ends and subjected to self-weight and tension T_1 at the top right end.

The geometric configuration of the static solution for the case of $T_1=1875\text{N}$ is shown in Figure 4.

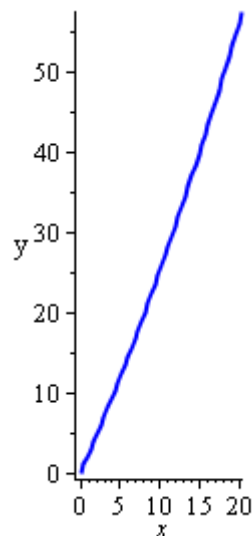


Figure 4: Geometric configuration of the static solution of a suspended cable subjected to an initial tension $T_1=1875\text{N}$

For comparison, the differential equations governing of this problem (catenary equation) derived by Pallares and Rodríguez (2008) were solved by a standard routine implemented in Maple and results, were coincident not shown here.

6.2 Example 2

Next the dynamic behavior of a taut cable is analyzed. The following data are adopted: $a = 20.40\text{m}$, $b = 57.70\text{m}$, $\Omega = 1.25 \times 10^{-4} \text{m}^2$, $L_0 = 56.6972$ $\omega_x = 0.1 \text{rad/s}$

$$f_1(t) = a - 0.07(1 - \cos(\omega_x t)), \quad f_2(t) = 0, \quad E = 1.6 \times 10^{11} \text{N/m}^2, \quad K = E\Omega,$$

$$\gamma_0 = \rho_0 g = 78500 \text{N/m}^3, \quad q_h = q_v = 0, \quad T_1 = 15000 \text{N}.$$

To find the Karhunen-Loève basis, a similar problem of a chain with 39 intermediate concentrated mass particles joined by springs (40 elastic links) is analyzed. The data matrices $\tilde{\mathbf{X}}$ and $\tilde{\mathbf{Y}}$ correspond to the geometric configuration of the chain (instantaneous horizontal and vertical coordinates at each mass particle) at 125 instants spaced 1 seconds.

In order to obtain eigenmodes with higher energy contribution (i.e. ε_i defined in Section 5) we need to construct the covariance matrix of the velocity field correlating all points in the domain. Assuming that the total number of points in space is n , then, the covariance matrix is $(n \times m)$. In this work, we employ the snapshot method of Sirovich (1987b). Then,

$$\mathbf{X} = \begin{bmatrix} x_{11} & \cdots & \cdots \\ \cdots & \cdots & \cdots \\ x_{n1} & \cdots & \cdots \end{bmatrix} \quad (31)$$

Being n the number of mass particles and m the number of observations, x_{ij} and y_{ij} the spatial coordinates of the mass particle i at the time j . In this case, $n=41$ and $m=125$. The average of these data is given by

$$\boldsymbol{\mu}_x = \begin{bmatrix} \mu_{x,1} \\ \vdots \\ \mu_{x,n} \end{bmatrix} = \frac{1}{m} \begin{bmatrix} \sum_{i=1}^m x_{1i} \\ \vdots \\ \sum_{i=1}^m x_{ni} \end{bmatrix}, \quad \boldsymbol{\mu}_y = \begin{bmatrix} \mu_{y,1} \\ \vdots \\ \mu_{y,n} \end{bmatrix} = \frac{1}{m} \begin{bmatrix} \sum_{i=1}^m y_{1i} \\ \vdots \\ \sum_{i=1}^m y_{ni} \end{bmatrix} \quad (32)$$

In order to use Eqs. (29) the following matrices are introduced:

$$\bar{\mathbf{X}} = \begin{bmatrix} x_{11} - \mu_{x1} & \cdots & \cdots \\ \cdots & \cdots & \cdots \\ x_{n1} - \mu_{xn} & \cdots & \cdots \end{bmatrix} \quad (33)$$

Thus, data are now centered.

Recall that the governing equations for the problem of the extensible cable are given by

$$\begin{aligned} [x'(\xi^2 - 1)]' &= \frac{2}{K}(\rho_0 \Omega^2 \dots) \\ [y'(\xi^2 - 1)]' &= \frac{2}{K}(\rho_0 \Omega^2 \dots J - q_v) \end{aligned} \tag{34}$$

With $x(0, t) = 0, y(0, t) = 0, x(L_0, t) = f_1(t), y(L_0, t) = f_2(t)$. The following change of variables is introduced

$$\begin{aligned} \hat{x} &= x(X, t) - \frac{X}{L_0} f_1(t) \\ \hat{y} &= y(X, t) - \frac{X}{L_0} f_2(t) \end{aligned} \tag{35}$$

System (35) governs the problem along with the boundary conditions (BC) which are $\hat{x}(0, t) = \hat{x}(L_0, t) = 0$ and $\hat{y}(0, t) = \hat{y}(L_0, t) = 0$. With this change of variables the basis functions hold the BC at every instant. From the matrices $\hat{\mathbf{X}}$ and $\hat{\mathbf{Y}}$ ($\bar{\mathbf{X}}$ and $\bar{\mathbf{Y}}$ matrices expressed in the new variables), the Karhunen-Loève basis $\{\hat{\phi}_{xi}(X)\}_{i=1..m}, \{\hat{\phi}_{yi}(X)\}_{i=1..n}$ are already expressed in the new variables. The differential system is solved by means of a Galerkin approach where the unknown functions are approximated by the expressions:

$$\begin{aligned} \hat{x} &= \bar{x}(X) + \sum_{i=1}^r a_i(t) \phi_{xi}(X) \\ \hat{y} &= \bar{y}(X) + \sum_{i=1}^r b_i(t) \phi_{yi}(X) \end{aligned} \tag{36}$$

Where $\bar{x}(X)$ and $\bar{y}(X)$ are the average values of $\hat{x}(X, t)$ and $\hat{y}(X, t)$. $\hat{\phi}_{xi}(X)$ and $\hat{\phi}_{yi}(X)$ are the KL basis (POMs), a_i and b_i are unknown.

The first five singular values that characterize the dynamics of the chain are given in Table 2.

From the sum of all proper orthogonal values $\sum_{r=1}^i \sigma_{xi} = 7.1486$ and $\sum_{r=1}^i \sigma_{yi} = 2.516$ respectively, with ($r = 20$), it can be seen that only one POV is enough to capture more than 95% of the "energy" contained in the data.

σ_{xi}	$\sum_{r=1}^i \varepsilon_{xi} (\%)$	σ_{yi}	$\sum_{r=1}^i \varepsilon_{yi} (\%)$
6.8343	95.60	2.40026	95.49
0.1963	98.35	0.0711	98.32
0.0842	99.52	0.0296	99.50
0.0133	99.71	0.0047	99.69
0.0058	99.80	0.0024	99.79

Table 2: Proper orthogonal values for the horizontal and vertical motion. Percent of total energy captured by each POV

In Figure 5 the empirical eigenfunctions (POMs) corresponding to the first three POVs of $\hat{\mathbf{X}}$ are shown.

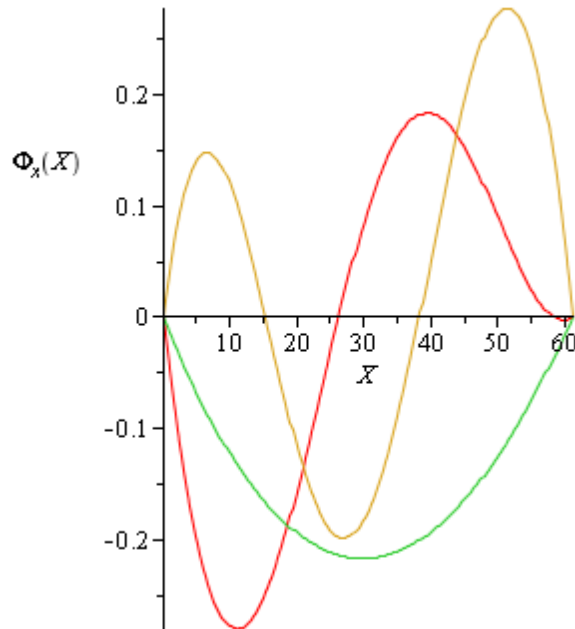


Figure 5: First three Proper orthogonal modes. Example 2

In Figure 6 a snapshot of the geometric configuration of the cable is shown for instant $t = 45$ s. As it can be seen, it is enough only one POMs from the KL Basis to capture a good characterization of the cable dynamic. Again as it was expected and as it was verified in a previous work (Escalante, 2008), the dynamic behavior of a cable and a chain with large number of links are similar.

6.3 Example 3

Next example, a cable dynamic whose right top end describes a higher frequency motion is analyzed. The following data are adopted: $a = 20.40$ m, $b = 57.70$ m, $\Omega = 1.25 \times 10^{-4}$ m², $L_0 = 58.9937$ (Pre-tension $T_1 = 3750$ N), $\omega_x = 0.5$ rad/s, $f_1(t) = a - 0.07(1 - \cos(\omega_x t))$, $f_2(t) = 0$, $K = EA$, $\gamma_0 = \rho_0 g = 78500$ N/m³, $E = 1.6 \times 10^{11}$ N/m², $q_h = q_v = 0$.

In this case the percents of the energies contained in the data captured by the first five POVs are 85.66% and 85.70% for the horizontal and vertical motions respectively.

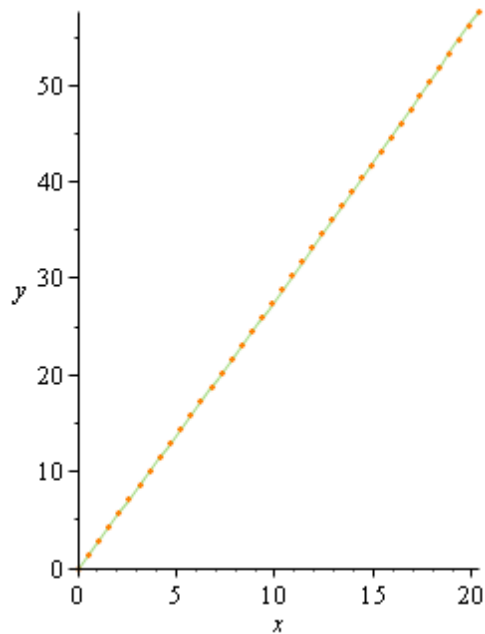


Figure 6: Snapshot of the geometric configuration at $t = 15s$ for the cable and a chain of 40 elastic linktion aproximante, using one POM for the approximating solution.

In Figure 7 the trajectory described by the cable is shown through six snapshots at the instants $t = 0, 15, 30, 45, 60$ and 90 seconds. Finally, in Figure 8 a snapshot of the geometric configuration of the cable for instatnt $t = 45s$ is shown.

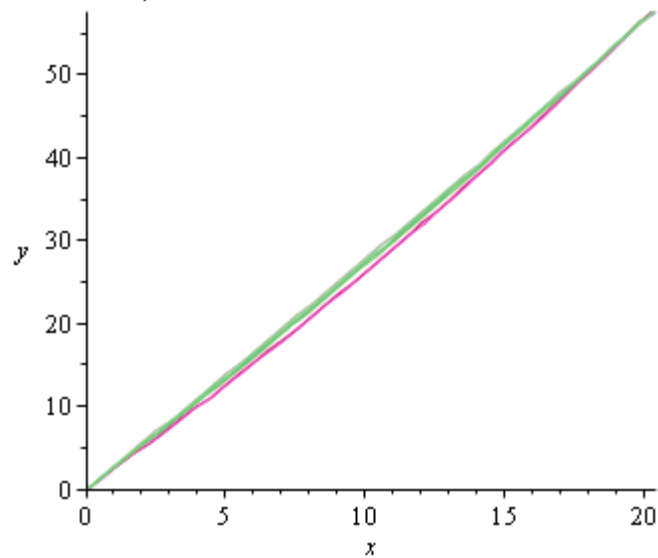


Figure 7: Trajectory described by a cable with a prescribed motion at the ends. Example 3.

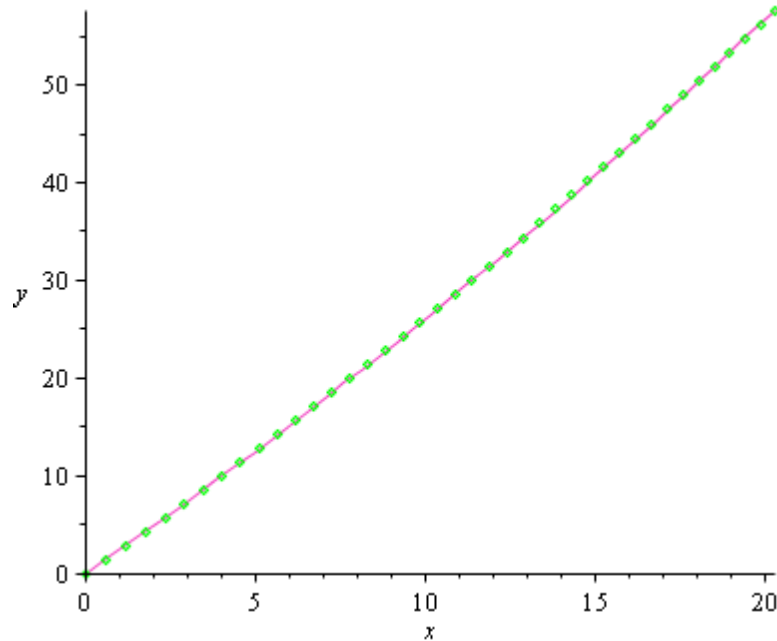


Figure 8: Geometric configuration for instant $t = 45s$, for the dynamic of an elastic chain (points line) and of a cable (continued line) using two approximating functions (POMs) for the solution. Example 3.

6.4 Example 4:

Now, in this example the behavior of a suspended cable with prescribed motions at ends and uniform horizontal and vertical loads is shown. The following data are adopted: $a = 20.40m$, $b = 57.70m$, $\Omega = 1.25 \times 10^{-4} m^2$, $L_0 = 60.1479$, $T_1 = 7500N$, $\omega_x = 0.3 rad/s$, $f_1(t) = a - 0.07(1 - \cos(\omega_x t))$, $f_2(t) = 0$, $E = 1.6 \times 10^{11} N/m^2$, $\rho_0 = 78500 N/m^3$, $q_h = 1.5 \rho_0 \Omega g$.

Again, for comparison, results obtained from the dynamic analysis of an elastic chain and of a extensible cable using KL Basis are shown in Figure 9.

7 CONCLUSIONS

In the present work an interesting and advantageous technique to solve dynamic of extensible taut cables was shown. Starting from the knowledge of a problem with similar characteristics, though simpler (the dynamics of an extensible chain), the behavior of an extensible cable could be analyzed. For a cable with a standard stiffness and a chain with a large number of links (particle masses joined by springs), it was proved that the dynamic behavior in both cases is similar as depicted.

Proper orthogonal decomposition is a methodology that firstly identifies the modes with larger "energy" in an evolving system, and secondly provides a means of obtaining a low-dimensional description of the system dynamics.

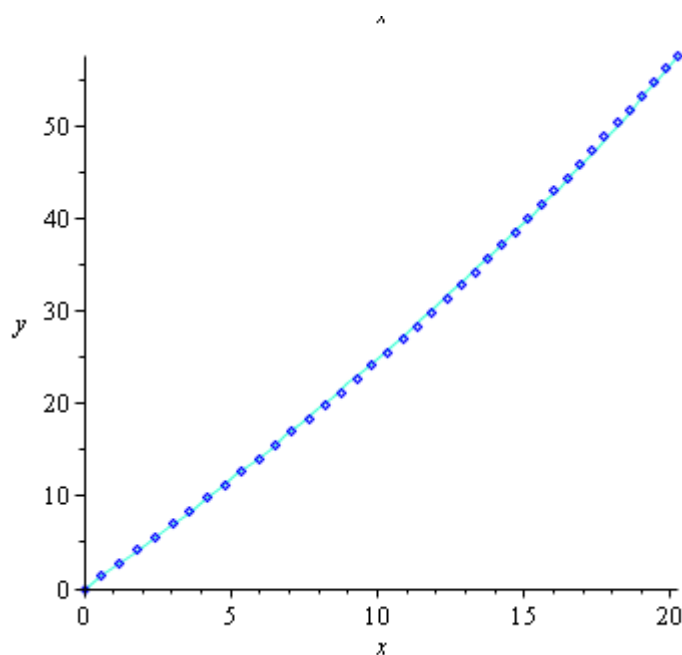


Figure 9: Snapshot of the geometric configuration at $t = 45s$, of the chain (dot line) 40 elastic links and of the cable (continued line) using three approximating functions (POMs) for the solution.

The proper orthogonal decomposition method was used to find the set of orthogonal functions to use then as trial functions with the Galerkin Method. The basis, obtained in this way (Karhunen-Loève Basis) are, as known, optimal since they provide the best approximation to the real solution in the sense of the minimum square. It could be seen, as well, that the first proper orthogonal values (POVs) accumulate a great percent of the energy contained in the dynamic and because of that, few functions are enough to get a good approximation to represent the real solution.

It is important to remark the fact that solving an ordinary differential problem (chains), a more complex problem governed by partial differential equations could afterwards be analyzed.

REFERENCES

- Chatterjee A., An introduction to the proper orthogonal decomposition. *Current Science*. 78:808-817, 2000.
- Escalante M.R., Rosales M.B, Filipich C.P, Planteo y solución del problema de amarres no lineales de una plataforma flotante. *Mecánica Computacional*. 24:785-796, 2005.
- Escalante M.R., Rosales M.B, Filipich C.P., Sampaio R., Análisis dinámico de cables extensibles poco tensos: método de descomposición ortogonal propia. *Mecánica Computacional*, 27:771-784, 2008.
- Filipich C. and Rosales M., A further study on the postbuckling of extensible elastic rods. *International Journal of Non-Linear Mechanics*, 35: 997-1002, 2000.

- Glösmann, P. and Kreuzer, E., Nonlinear systems analysis with Karhunen-Lòeve transform. *Nonlinear Dynamics*, 41: 111-128, 2005.
- Hagedorn, P. and Schafer, B., On non-linear free vibrations of an elastic cable, *International Journal of Non-Linear Mechanics* 15:333-340, 1980.
- Holmes P., Lumley J.L. and Berkooz G., Turbulence, Coherent Structures, *Dynamical Systems and Symmetry*. Cambridge University Press. 1996.
- Hotelling H., Analysis of a complex of statistical variables into principal components. *Journal of Educational Psychology*. 24:417-441, 498-520, 1933.
- Ibrahim R.A., Nonlinear dynamics of suspended cables. Part III: Random excitation and interaction with fluid flow. *ASME Applied Mechanics Reviews*, 57:515-549, 2004.
- Irvine H.M., *Cable Structures*. MIT Press, Cambridge, 1981.
- Irvine H.M. and Caughey T.K., The linear theory of free vibrations of a suspended cable. *Proceedings of the Royal Society of London*, A341:299-315, 1974.
- Karhunen K, Zur Spektraltheorie Stochastischer Prozesse. *Annals of Academic Science Fennicae*, Series A1 Mathematics and Physics 37, 1946.
- Kerschen, G., Golinval, J., Vakakis, A. and Bergman, L., The method of proper orthogonal decomposition for dynamical characterization and order reduction of mechanical systems: an overview. *Nonlinear Dynamics*, 41: 147-169, 2005.
- Kosambi D., Statistics in function space. *Indian Math Soc.*, 7:76-88, 1943.
- Leonard, J.W., *Tension Structures: Behaviour and Analysis*. McGraw Hill, New York, 1988.
- Liang Y., Lee H., Lim S., Lin W. Lee K. and Wu C. Proper orthogonal decomposition and its applications – Part I: Theory. *Journal of Sound and Vibration*. 252:527-544, 2002.
- Loève M., *Fonctions Alatoires du Second Ordre. Processus stochastiques et mouvement Brownien*, Ed. P. Levy, Paris, 1948.
- Luongo A., Rega G. and Vestroni F., Planar non-linear free vibrations of an elastic cable. *International Journal of Non-Linear Mechanics*, 19:39-52, 1984.
- Obukhov M., Statistical description of continuous fields, *T. Geophys. Int. Akad. Nauk., USSR*. 24, 3-42, 1954.
- Pallares Muños M.R. and Rodríguez Calderón W., Validación de la formulación numérica de la catenaria elástica con Ansys. *Matemáticas: Enseñanza Universitaria*. 16:63-85, ISSN 0120-6788. Universidad del Valle, Colombia, 2008.
- Pearson K., On lines and planes of closest fit to systems of points in space. *Philosophical Magazine*, 2(6): 559-572, 1901.
- Pougachev V., General theory of the correlations of random functions. *Izv. Akad. Nauk. USSR*. 17: 1401-1402, 1953.
- Rega G. Nonlinear dynamics of suspended cables, Part I: Modeling and analysis; Part II: Deterministic phenomena, *ASME Applied Mechanics Reviews*, 57:443-514, 2004.
- Rega G. and Luongo A., Natural vibrations of suspended cables with flexible supports. *Computers & Structures*, 12:65-75, 1980.

- Rega G., Vestroni F. and Benedettini F. Parametric analysis of large amplitude free vibrations of a suspended cable. *International Journal of Solids and Structures*, 20:95-105, 1980.
- Rosales M.B., Filipich C.P., Escalante M.R., Dinámica de una estructura flotante amarrada: modelado de la no linealidad mediante recurrencias algebraicas. *Mecánica Computacional*, 22:1051-1063, 2003.
- Sirovich L., Turbulence and the dynamics of coherent structures - Part I: coherent structures. *Quarterly of Applied Mathematics*, 45(3): 561-571, 1987a.
- Sirovich L., Turbulence and the dynamics of coherent structures - Part II: symmetries and transformations. *Quarterly of Applied Mathematics*, 45(3): 573-582, 1987b
- Sirovich L., Turbulence and the dynamics of coherent structures - Part III: dynamic and scaling. *Quarterly of Applied Mathematics*, 45(3): 583-590, 1987c
- Takahashi K. and Konishi Y., Nonlinear vibrations of cables in three dimensions, part I: nonlinear free vibrations. *Journal of Sound and Vibration*, 118:69-84, 1987.
- Triantafyllou, M.S., Linear dynamics of cable and chains. *Shock and Vibration Digest*, 16:9-17, 1984.
- Triantafyllou, M.S., Dynamics of cables and chains. *Shock and Vibration Digest*, 19:3-5, 1987.
- Wilson H., Turcotte L., Halpern D. Advanced mathematics and mechanics applications using MATLAB, CRC press, 2003.